Noninvasive Breathing Effort Estimation of Mechanically Ventilated Patients Using Sparse Optimization

JOEY REINDERS [1,2], **BRAM HUNNEKENS** [1], **NATHAN VAN DE WOUW** [2,3] **(Fellow, IEEE),**
AND TOM OOMEN [2,4] **(Senior Member, IEEE)**

[1]Demcon Advanced Mechatronics, Best, 5600, MB Eindhoven, Netherlands
[2]Department of Mechanical Engineering, Eindhoven University of Technology, 5612, AZ Eindhoven, Netherlands
[3]Department of Civil, Environmental and Geo-Engineering, University of Minnesota, Minneapolis, MN 55455 USA
[4]Delft Center for Systems and Control, Delft University of Technology, 2628, CD Delft, Netherlands

CORRESPONDING AUTHOR: JOEY REINDERS (e-mail: joey.reinders@demcon.com).

ABSTRACT Mechanical ventilators facilitate breathing for patients who cannot breathe (sufficiently) on their own. The aim of this paper is to estimate relevant lung parameters and the spontaneous breathing effort of a ventilated patient that help keeping track of the patient's clinical condition. A key challenge is that estimation using the available sensors for typical model structures results in a non-identifiable parametrization. A sparse optimization algorithm to estimate the lung parameters and the patient effort, without interfering with the patient's treatment, using an ℓ_1-regularization approach is presented. It is confirmed that accurate estimates of the lung parameters and the patient effort can be retrieved through a simulation case study and an experimental case study.

INDEX TERMS ℓ_1-regularization, mechanical ventilation, parameter estimation, respiratory systems, system identification.

I. INTRODUCTION

Mechanical ventilation is a life-saving therapy used in Intensive Care Units (ICUs) to assist patients who need support to breathe sufficiently. The main goals of mechanical ventilation are to ensure oxygenation and carbon dioxide elimination [1]. Especially during the flu season or a world-wide pandemic such as the COVID-19 pandemic [2], mechanical ventilation is a life saver for many patients around the world.

Accurately tracking the patient's clinical condition is essential to optimize the patient's treatment. A lung model, e.g., a linear one-compartmental lung model [3, pp. 37–60], can be estimated to retrieve valuable information about the patient's clinical condition. These estimates give an indication of the lung compliance, i.e., the inverse of the lung stiffness, and the resistance of the patient's airway. In [4] and [5], such parameters have been estimated during ventilation of *fully sedated patients* using recursive least squares algorithms. However, during the weaning process the assistance delivered by the ventilator is reduced gradually and the patient is *breathing*

spontaneously as well. This breathing effort causes the estimated patient models to be inaccurate and practically useless if this effort is not taken into account. Furthermore, if the breathing effort is not considered in the treatment it might result in critical volutrauma and thus severely harm the patient. Also, an accurate estimate of the patient effort can be used to detect, and eventually prevent, patient-ventilator asynchrony. According to [6], this patient-ventilator asynchrony is associated to increased mortality. Therefore, accurate estimates of this effort and the patient parameters are relevant to determine the patient's clinical condition and improve the patient's treatment.

Two distinct types of methods can be distinguished to obtain the desired patient information in case of *spontaneously breathing patients*. First, methods that are employing additional sensing equipment are available. The required additional sensors makes these methods less attractive for widespread use in all ICUs, because placing additional sensors is error-prone and it demands more time of the ICU

personnel. This is undesired because the ICUs are already understaffed [7], [8]. Second, algorithms that use the already available data in ventilation are available. Typically, these methods impose an extra maneuver, i.e., an additional change in pressure, or some assumption on the patient effort. Next, both such approaches are investigated in detail.

The first class of methods, requiring additional sensing, are error-prone and costly in terms of personnel time. Next, methods requiring additional sensing are presented. In Neurally Adjusted Ventilatory Assist (NAVA), [9]–[11], an invasive esophagus catheter is used to measure diaphragm activity. Using an esophagus catheter is both invasive and error-prone [12]. Therefore, it is not suitable for many patients. In [13], non-invasive surface electromyography (EMG) measurements are used to estimate the patient's breathing effort. The presented methods all require additional, possibly invasive, sensing. This is undesired because it costs valuable time of the ICU personnel and is error-prone.

The second class of methods do not require additional sensing, yet are highly challenging from an estimation perspective, typically imposing unrealistic restrictions on the patients breathing effort. In [14] and [15], a method is presented to estimate the patient parameters and effort during ventilation. These methods assume that the change in patient effort over successive breaths is insignificant and require an extra maneuver, interfering with the treatment. Therefore, they are not preferred in practice. In [16]–[19], a method that estimates the lung impedance of a spontaneously breathing patient by superimposing a multi-sine to the pressure target is developed. To extract the patient effort from the actual signal, the patient is requested to breathe with a specific frequency. In critically ill patients, it is typically not possible to demand this from a patient. Another disadvantage of this method is that it interferes with the treatment. Besides critically ill patients, this Forced Oscillation Technique (FOT) method has also been applied to COPD patient's to distinguish different types of COPD in [20]. In [21], a method to estimate the lung elastance of spontaneously breathing patients is proposed. This method makes a reconstruction of the measured airway pressure, as if no patient breathing effort is present. This reconstructed pressure is used to estimate the elastance. It clearly shows an improved elastance estimate. However, no realistic time-varying patient effort is obtained. In [22], strictly negative b-spline basis functions are used to model the patient effort. Using these basis functions, the patient's effort, lung elastance, and lung resistance are estimated. This method shows good results of the estimated effort. A drawback of this method is that the distribution of the basis functions does not allow for breathing effort at the end of the ventilator-induced breath. In [23], it is assumed that the patient effort first monotonically increases and thereafter monotonically decreases to zero. We believe that this limitation on the patient effort is too stringent in practice. In [24], several different methods to estimate lung dynamics of sedated and spontaneously breathing patients are compared. It is shown to be challenging to obtain constant estimates in case of spontaneous breathing effort.

In conclusion, the presented methods are able to retrieve valuable information about the patient's lung parameters and the patient effort. However, they restrict the estimated patient effort and interfere with the treatment.

Although several estimation algorithms have been developed that improve the estimation of patient effort and a patient model, these all require either more data, an extra maneuver, or use rather stringent assumptions on the patient effort. Indeed, in [25] and [26], it is concluded that there is no consensus on how patient effort should be modeled. However, from a practical point of view it is valid to assume that the effort is not changing arbitrarily within a particular breath. More specifically, the patient effort has some smoothness properties and does not arbitrarily change slope or contain large steps. Note that the patient effort can change significantly over successive breaths. The smoothness property of the patient effort can be ensured by assuming that the second time derivative of the effort is sparse, i.e., it contains only a few non-zero elements. Therefore, in this paper estimation methods of sparse signals are considered as a possible solution to the estimation problem at hand. In particular, ℓ_0-regularization and its convex relaxation ℓ_1-regularization are considered in this paper. Such ℓ_1-regularization is used in for example the Least Absolute Shrinkage and Selection Operator (lasso) [27] and fused lasso [28]. These methods are used to compute sparse feedforward control signals [29] and to enhance sparsity in system identification [30], [31].

The main contribution of this paper is an estimation framework, using sparse optimization, that enables estimation of the patient effort and the patient's lung model of a mechanically ventilated patient with spontaneous breathing effort. The presented approach meets the following requirements: 1) it only uses commonly available data; 2) it does not use an extra ventilation maneuver; and 3) it leaves freedom regarding the shape of the patient effort. As subcontributions, the performance of this algorithm is investigated through a simulation case study and through an experimental setup with an actual ventilator and a mechanical lung.

The outline of this paper is as follows. In Section II, the considered patient model is presented. In Section III, the estimation goal and challenge are described in detail. Then, In Section IV, the proposed sparse estimation method is explained in detail. Thereafter, in Section V, a simulation case study is presented to analyze the performance of the algorithm. Then, in Section VI, an experimental case study is used to show the performance of the proposed algorithm in practice. Finally, in Section VII, the main conclusions and recommendations for future work are presented.

II. PATIENT AND BREATHING EFFORT MODELING
In this section, a description of the considered patient model is presented. In Section II-A, the considered patient model and its relevant parameters are presented. Thereafter, in Section II-B, the considered patient breathing effort model is presented.
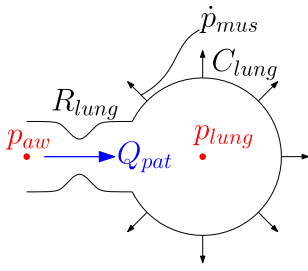
FIGURE 1. Schematic representation of the patient's respiratory system, with the relevant patient parameters and signals. The signals p_{aw} and Q_{pat} are typically measured during mechanical ventilation.

A. PATIENT MODEL

The model considered in this paper is a linear one-compartmental lung model, which is extensively described in [3, pp. 37–60]. An advantage of this model description is its ease of interpretation for clinicians and engineers. The linear one-compartment lung model has sufficient accuracy for our purpose, i.e., exposing clinically valuable information about the patient's state of health; hence a more complex model is not justified. In addition, this allows for parameters that are easy to interpret since the linear one-compartment lung model consists of two physical parameters, namely, the airway resistance and lung compliance.

Fig. 1 shows a schematic representation of the patient's respiratory system with the parameters and signals relevant for estimation. The patient model without patient effort consists of two components that are modeled; namely, the airway and the lungs. The airway model describes the relation between the pressure drop over the airway and the flow in and out of the patient's lungs. The lung model gives the relation between the flow in and out of the lungs and the pressure inside the lungs.

The airway is modeled by means of a linear resistance R_{lung}. This linear resistance gives the relation between the airway pressure, the lung pressure, and the patient flow:

$$Q_{pat}(t) = \frac{p_{aw}(t) - p_{lung}(t)}{R_{lung}}, \quad (1)$$

where p_{aw} is the airway pressure, the pressure near the patients mouth, and p_{lung} is the lung pressure, the pressure inside the lungs.

The lung model describes the relation between the patient volume V_{pat}, i.e., the volume inside the lungs, and the lung pressure p_{lung}. This relation is described by a linear lung compliance C_{lung}. The pressure inside the lungs is expressed as

$$p_{lung}(t) = \frac{1}{C_{lung}} \underbrace{\int_{t_0}^{t} Q_{pat}(\tau)d\tau}_{V_{pat}(t)} + p_{lung}(t_0) + p_{mus}(t), \quad (2)$$

where integration of the flow over time gives the patient volume V_{pat} and $p_{lung}(t_0)$ is the initial lung pressure at time t_0. Furthermore, p_{mus} describes the pressure fluctuation that is caused by the patient's spontaneous breathing effort, i.e., by contraction and relaxation of its respiratory muscles. This patient effort is modeled as an additive disturbance to the lung pressure. More details on the patient effort are presented in Section II-B.

Combining (1) and (2), and rewriting to a discrete-time equation gives the following expression for the airway pressure p_{aw}:

$$p_{aw}(k) = \frac{1}{C_{lung}} V_{pat}(k) + R_{lung} Q_{pat}(k)$$
$$+ p_{lung}(1) + p_{mus}(k), \quad (3)$$

where k denotes the discrete sample number and $p_{lung}(1)$ denotes the initial lung pressure. Eventually, (3) is used in the cost function of the estimation algorithm in Section IV. The considered patient effort model is investigated in the next section.

B. PATIENT EFFORT MODEL

Patient effort enables a person, i.e., healthy person or sick patient, to inhale and exhale air by themselves. In this section, the most important properties of the patient effort are presented. Further, it is explained how these properties are translated to a model of the patient's spontaneous breathing effort. This model is a time-series describing the exogenous pressure disturbance $p_{mus}(t)$ on the lung pressure $p_{lung}(t)$. Physically, the patient effort can be seen as a change in lung pressure caused by contractions and relaxation of the respiration muscles, e.g., the diaphragm. For example, contraction of the diaphragm results in a downward motion of the diaphragm. This motion results in a pressure drop in the lungs. Various other approaches are currently being used to model the patient effort. For example using a time-varying lung elastance in [32], [33], we believe that the method adopted in this paper is the most intuitive. Based on physical properties of respiration, two assumptions on the shape of patient effort are made in this section. Furthermore, a commonly used patient effort model is briefly presented.

Firstly, the assumption is made that the modeled patient effort $p_{mus}(t)$ is non-positive. In [22], this same assumption is adopted and it is shown that this can give realistic estimates in a large group of patients. Typically inspiration is an active process, where the diaphragm is contracted. This results in a decrease in lung pressure. This decrease in lung pressure is modeled by a negative patient effort $p_{mus}(t)$. Expiration is typically a passive process, where the respiration muscles are relaxing and the elasticity of the lungs result in a negative airflow. Expiration is modeled by increasing the negative patient effort until it is zero again. Because expiration is typically passive, Assumption 1 is adopted throughout this paper.

Assumption 1: The patient effort $p_{mus}(t)$ is a non-positive signal, i.e.,

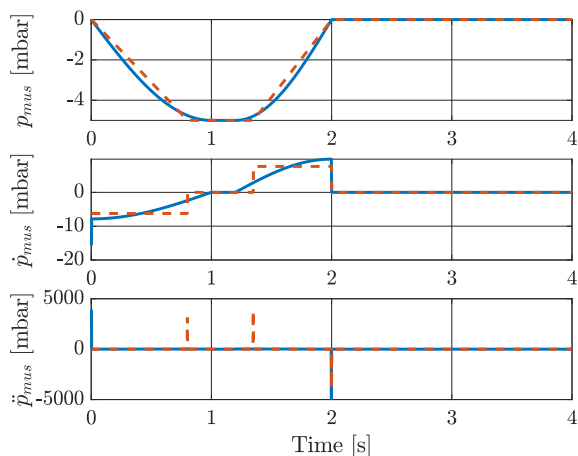$$p_{mus}(t) \leq 0, \forall t \geq 0. \quad (4)$$

FIGURE 2. Example of a model for the patient effort $p_{mus}(t)$ and its first and second time derivatives. A sinusoidal half-wave (——) and a piecewise linear (- - -) patient effort model are shown.

FIGURE 3. Schematic example of PC-ASV. The figure shows the target pressure (——), the measured airway pressure p_{aw} (——) and patient flow Q_{pat} (——), and the patient effort p_{mus} (——).

Secondly, it is assumed that the shape of the modeled patient effort $p_{mus}(t)$ cannot change arbitrarily within one breath. However, the patient effort is allowed to change arbitrarily over successive breaths. According to [26], it is common to use a sinusoidal half-wave for the patient effort. An example of the sinusoidal half-wave and a piecewise linear version of the effort, and their first and second time derivatives are depicted in Fig. 2. It is shown that a piecewise linear effort gives a fairly accurate representation of the sinusoidal half-wave. Furthermore, it is observed that the second time-derivative of the piecewise linear $p_{mus}(t)$ is sparse, i.e., it only contains a few non-zero elements. This sparsity property of $\ddot{p}_{mus}(t)$ is used as prior knowledge in the estimation algorithm, without fixing the exact timing and height of the signal. Using the presented patient models, the estimation goal and the main challenge are presented in the next section.

III. ESTIMATION GOAL

In this section, the estimation goal is presented. Then, the practical estimation setting with its limitations and constraints is presented. Finally, the main challenge is presented.

The estimation goal is to retrieve accurate estimates of the patient's breathing effort, $p_{mus}(t)$, the lung compliance C_{lung}, and the patient's resistance R_{lung}. Accurate estimates of these parameters can be used to follow the patient's clinical condition and adjust the treatment accordingly. From discussions with experts in the field it is concluded that an accuracy of about 15% of the compliance and resistance estimates is practically useful and therefore desired. Therefore, the requirement for estimation accuracy of the lung parameters is 15%. The estimation goal must be achieved by using the typically measured signals, i.e., airway pressure $p_{aw}(t)$, the patient flow $Q_{pat}(t)$, and the patient volume $V_{pat}(t) = \int_{t_0}^{t} Q_{pat}(\tau)d\tau$.
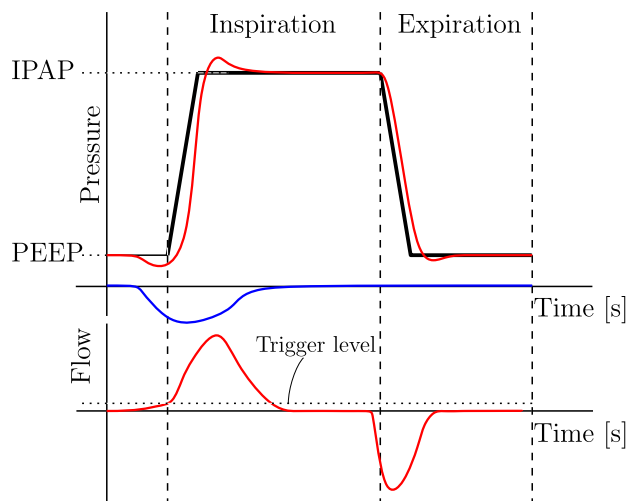
The considered estimation setting is a particular ventilation mode, namely, Pressure Controlled - Assist Control Ventilation (PC-ACV), schematically depicted in Fig. 3. The figure shows the airway pressure p_{aw}, patient flow Q_{pat}, and patient effort p_{mus} during one breath of triggered ventilation. The ventilator is detecting the start of the patient effort to synchronize the machine with the patient. Typically the start of inspiration is detected by detecting an increase in the patient flow. This patient flow is caused by the patient's inspiration effort. When the start of the patient's effort is detected, a breath cycle of the mechanical ventilator is started to assist the patient. This a breath cycle is induced by increasing the patient's airway pressure p_{aw} to the Inspiratory Positive Airway Pressure (IPAP) level. The pressure level generated by the mechanical ventilator is lowered after a preset time to the Positive End-Expiratory Pressure (PEEP) level to allow the air to leave the patient's lungs in the expiration phase. Note that the application of the algorithm developed in this paper is not limited to this single ventilation mode and can be used in combination with a variety of ventilation modes. The main constraint is that the ventilation modes where it can be applied require a significant known external excitation by the ventilator, i.e., in its current form the algorithm does not work for Continuous Positive Airway Pressure (CPAP) ventilation. Examples of modes that contain such known external excitation by the ventilator are: Assist Control Ventilation (ACV), Continuous Mandatory Ventilation (CMV), and Continuous Spontaneous Ventilation (CSV).

Next, an assumption on the breathing effort and a restriction on the target pressure are presented. First, it is assumed that the patient effort can significantly change from breath to breath. It might change in breath depth, i.e., amplitude, as well as in shape such as timing, rise times, and length. This means that the estimation algorithm should be able to deal

with such changes. Second, it is desired not to interfere with the treatment. Therefore, it is undesired to change the target pressure to obtain estimates of the patient parameters, i.e., it is not allowed to add an extra maneuver to the ventilator.

The main challenge in estimating physically interpretable parameters is the non-identifiability of the estimation problem. More specifically, the relation between the airway pressure, patient flow, and patient volume, given by (3) has infinitely many solutions, i.e., infinitely many combinations of the estimates, $\hat{C}_{lung}$, $\hat{R}_{lung}$, $\hat{p}_{lung}(1)$, and $\hat{p}_{mus}(k)$ with $k \in [1, N]$, describe the relation between the measured signals. This can be seen by writing (3) as follows:

$$Y = X\beta, \tag{5}$$

where

$$Y = \begin{bmatrix} p_{aw}(1) \\ p_{aw}(2) \\ \vdots \\ p_{aw}(N) \end{bmatrix}, \beta = \begin{bmatrix} \frac{1}{C_{lung}} \\ R_{lung} \\ p_{lung}(1) \\ p_{mus}(1) \\ p_{mus}(2) \\ \dots \\ p_{mus}(N) \end{bmatrix}, \text{ and}$$

$$X = \begin{bmatrix} V_{pat}(1) & Q_{pat}(1) & 1 & 1 & 0 & \dots & 0 \\ V_{pat}(2) & Q_{pat}(2) & 1 & 0 & 1 & \dots & 0 \\ \vdots & \vdots & \vdots & \vdots & \vdots & \ddots & \vdots \\ V_{pat}(N) & Q_{pat}(N) & 1 & 0 & 0 & \dots & 1 \end{bmatrix}.$$

Thus, in (5), Y reflects the measured airway pressure sampled at discrete time instants, X reflects, a.o., the measured patient volume and flow, and β represents the quantities to be estimated. Using this representation it can be shown that $X^T X$ is not invertible, hence, there exists an infinite number of solutions for β, β is not identifiable. This can also be understood intuitively; by considering the following simulation-error based least-squares cost function:

$$J = \sum_{k=0}^{k=N} (p_{aw}(k) - \hat{p}_{aw}(k))^2 \tag{6}$$

with k the sample index of the discrete signals, N the length of the signals in samples, and $\hat{p}_{aw}(k)$ defined as:

$$\hat{p}_{aw}(k) = \frac{1}{\hat{C}_{lung}} V_{pat}(k) + \hat{R}_{lung} Q_{pat}(k)$$
$$+ \hat{p}_{lung}(1) + \hat{p}_{mus}(k). \tag{7}$$

It is observed that independent of the choice of $\hat{C}_{lung}$, $\hat{R}_{lung}$, and $\hat{p}_{lung}(k)$ choosing $\hat{p}_{mus}(k) = p_{aw}(k) - (\frac{1}{\hat{C}_{lung}} V_{pat}(k) + \hat{R}_{lung} Q_{pat}(k) + \hat{p}_{lung}(1))$ results in $\hat{p}_{aw}(k) = p_{aw}(k), \forall k \geq 0$. Therewith, the cost function (6) is zero.

Because the relation between the measured signals is non-unique, prior knowledge enables obtaining sensible estimates of the desired parameters and the patient effort. In literature, extra sensing ([9]–[11], [13]), maneuvers ([14]–[17]), or stringent assumptions on the shape of the effort ([14], [15], [23]) are used to solve this challenge. However, from the earlier defined estimation setting, it is clear that this is practically undesired. More explicitly, using stringent constraints in the estimation algorithm could prevent the estimation algorithm from estimating the actual patient effort. Therefore, in the following section an estimation method is presented that does not require additional sensing or maneuvers and does not use unrealistically stringent constraints on the estimated patient effort. Note that we are not considering the effect noise in this estimation problem, so in fact it is a realization problem.

IV. SPARSE ESTIMATION

In the previous section, the main estimation challenge is presented, namely, the relation between the measured signals and the estimated parameters and signal is underdetermined. In this section, a simulation-error based estimation algorithm is presented that uses the properties of the patient effort in Section II-B to overcome the identifiability challenge of Section III.

In Section II-B, it is argued that the patient effort $p_{mus}(k)$ does not change arbitrarily. More specifically, at the end of Section II-B it has been argued and shown that the second time-derivative of the sinusoidal half-wave patient effort model, i.e., $\ddot{p}_{mus}(k)$, can be accurately modeled as a sparse signal. Furthermore, in many cases the patient effort can be modeled to be non-positive, as also proposed Assumption 1. Embedding these two assumptions on the shape of p_{mus} in an optimization problem enables us to use the following constrained optimization problem:

$$\min_{\hat{C}_{lung}, \hat{R}_{lung}, \hat{p}_{lung}(1), \hat{p}_{mus}} \sum_{k=0}^{k=N} (p_{aw}(k) - \hat{p}_{aw}(k))^2$$

$$\text{subject to} \qquad \|\ddot{\hat{p}}_{mus}\|_0 \leq v$$

$$\hat{p}_{mus}(k) \leq 0 \forall k, \tag{8}$$

where $\|\ddot{\hat{p}}_{mus}\|_0$ represents the cardinality function of $\ddot{\hat{p}}_{mus}$ which denotes the number of non-zero elements in $\ddot{\hat{p}}_{mus}$ and v gives the upper limit on the number of non-zero elements in $\ddot{\hat{p}}_{mus}$, i.e., the first inequality constraint in (8) enforces the sparsity property.

However, inclusion of such sparsity constraint in the optimization problem leads to a non-convex optimization problem, which is NP-hard [34]. To solve this problem, the cost-function should be minimized with all possible combinations of nonzero elements in p_{mus}. This renders the optimization problem not appealing from a computational point of view. The ℓ_1 norm $\| \cdot \|_1$ is a convex relaxation of the cardinality function $\| \cdot \|_0$, making it much more attractive from a computational point of view. The ℓ_1 norm of $\ddot{\hat{p}}_{mus}$, denoted by $\|\ddot{\hat{p}}_{mus}\|_1$, is defined as the sum of absolute values of $\ddot{\hat{p}}_{mus}$. From [29] and [35], it is well known that inclusion of this ℓ_1 norm also enhances sparsity of $\ddot{\hat{p}}_{mus}$. Applying this relaxation and rewriting it with the Lagrange multiplier

λ gives the following regularized optimization problem:

$$\min_{\hat{C}_{lung},\hat{R}_{lung},\hat{p}_{lung}(1),\hat{p}_{mus}} \sum_{k=0}^{k=N} (p_{aw}(k) - \hat{p}_{aw}(k))^2$$

$$+\lambda\|\hat{\hat{p}}_{mus}\|_1$$

$$\text{subject to} \qquad \hat{p}_{mus}(k) \leq 0 \forall k, \quad (9)$$

where λ is a weighting parameter.

Note that in case the patient does actively exhale and the non-positivity constraint is violated, the estimates will be biased to compensate for this. In future research, after clinical validation of the current algorithm, the algorithm could be extended to handle non-positive p_{mus} values, e.g., by adding a cost penalizing positive values of p_{mus}.

Furthermore, the regularized optimization problem in (9) results in biased estimates, in literature this is referred to as shrinkage [36]. More specifically, when estimating the patient model and breathing effort perfectly the regularization term will result in a cost unequal to zero. Therefore, this regularization term will introduce some bias in the estimates. To reduce this bias, the retrieved values for $\hat{\hat{p}}_{mus}$ can be used to select the set of non-zero elements in $\hat{p}_{mus}$. This subset can be used in a re-estimation procedure to retrieve an estimate with a reduced bias. More specifically, the bias caused by shrinkage can be eliminated. This re-estimation method is also used in [29] to eliminate the bias in the estimated feedforward control signals when using sparse iterative learning control. The shrinkage of the parameters in this paper is limited, and therefore we have decided not to describe re-estimation technically. It can in some cases improve the estimates in view of (6) if the shrinkage is large. Because shrinkage is insignificant in the current case-study we left this re-estimation method as a recommendation which can be used to further improve estimation quality in future work or in other applications. The main motivation for using the ℓ_1 norm is that it provides a convex relaxation of the ℓ_0 norm. The question whether the right sparse vector is retrieved using (9) remains. In [37], a sufficient condition that relies on the restricted isometry property is provided. However, these conditions are violated in many practical cases. Nonetheless, the ℓ_1 norm provides an effective way to ensure sparsity.

To solve the optimization problem in (9), CVX has been used. CVX is a package for specifying and solving convex programs [38] and [39]. More specifically, to eventually solve the problem, CVX embedded the semi-definite programming solver SDPT3, which uses infeasible path-following algorithms to solve (9).

V. SIMULATION CASE STUDY

In this section, the presented approach is validated using simulations and it is compared to a least-squares estimator assuming zero patient effort. In Section V-A, the considered use-cases are briefly explained. Thereafter, the estimation results are presented and analyzed in Section V-B.
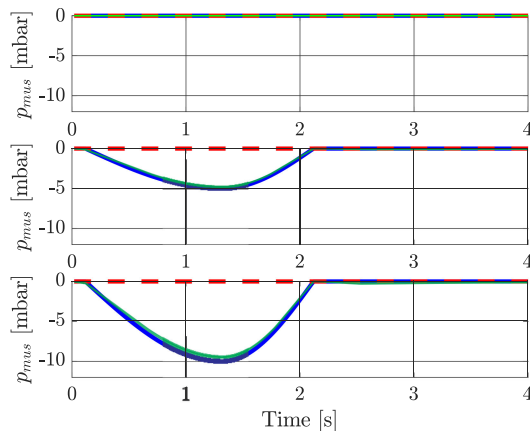

FIGURE 4. The true and estimated effort for every patient in simulations. From top to bottom the figures show the patients with a breath depth of 0, 5, and 10 mbar, respectively. The figures show the patient effort (——), the patient effort considered by the algorithm assuming $p_{mus} = 0$ (——), and the estimated effort using the presented approach (——).

A. SIMULATION CASE DESCRIPTION

In the simulations, a single-hose ventilation setup is considered, as in [40]. A single-hose ventilation system is considered because it simplifies modeling, since no expiration valve is used. Moreover, the developed algorithm only uses the pressures and flows measured near the patient, the algorithm's performance should be independent of the system that generates these signals. The inspiration time by the ventilator imposed breath is 2 seconds and the values for PEEP and IPAP are 5 and 20 mbar, respectively. The imposed breath cycle of the mechanical ventilator is triggered by the patient effort. In this simulation case study, it is assumed that the inspiration start of the ventilator and the patient are exactly synchronized. The data used for the optimization is sampled at 50 Hz.

In this simulation case study, four different patients and three different depths of patient effort are considered. The resistances R_{lung} of 5 and 10 mbar/l/s, and compliances C_{lung} of 20 and 50 ml/mbar are considered. The four considered patient models are obtained by all four possible combinations of these resistances and compliances. These patient types are based on the ISO standards for ventilation systems, which are obtain from Table 201.104 in NEN-EN-ISO 80601-2-12:2011 (NEN, Delft, The Netherlands). Furthermore, every patient is simulated without effort, i.e., $p_{mus}(k) = 0, \forall k$, with a maximum effort of 5 mbar, i.e., $\min(p_{mus}) = -5$ mbar, and with a maximum effort of 10 mbar, i.e., $\min(p_{mus}) = -10$ mbar. The patient effort for all cases is shown in Fig. 4.

For these use cases, the presented approach of Section IV, described by the optimization problem in (9) is compared to a traditional least squares optimization algorithm assuming zero effort which is currently implemented in many ventilation systems. For the optimization problem in (9), $\lambda = 2.5 \times 10^{-3}$ is used. This value for λ is retrieved by tuning such that sufficient performance is achieved for a variety of use-cases. In the traditional least squares optimization approach, it is
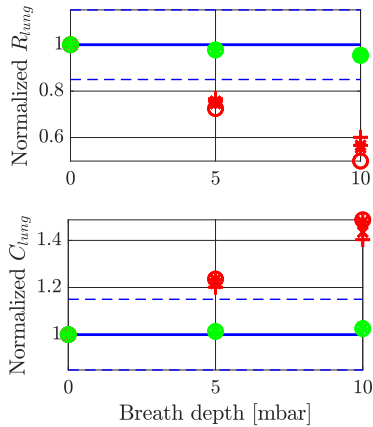
FIGURE 5. The normalized values of the estimated parameters $\hat{R}_{lung}$ and $\hat{C}_{lung}$ for the different patients against the breath depths in simulations. The figures show the true normalized parameters (———), the 15% accuracy interval (– – –), the estimated parameters neglecting the patient effort in red, and the estimated parameters using the presented approach in green. Four different patient types are considered namely: R5C20 (O), R10C20 (×), R5C50 (*), and R10C50 (+).

assumed that the patient effort is zero, i.e., $p_{mus} = 0 \forall k$, in the optimization problem given in (9).

We would like to stress that the considered model for the patient effort itself, i.e., the sinusoidal halfwave, does not completely satisfy the sparsity assumption in Section II-B. More specifically, the effort is retrieved by combining sine waves, of which the derivatives are by definition not sparse. Therefore, the simulation study in this section shows that the algorithm is able to retrieve valuable estimates in case the sparsity property for the patient effort is not completely satisfied.

B. SIMULATION RESULTS

The two main results are the improved estimation of the patient parameters and the estimation of patient effort compared to the traditional algorithm assuming zero patient effort. These main results are visualized in Figs. 4 and 5. In the remainder of this section, the results for the estimated parameters and the estimated patient effort are investigated separately. Then, a Monte Carlo study is performed to show that the proposed algorithm obtains accurate estimates for a wide variety of parameters and ventilation settings. Finally, in Section V-C the algorithm is used to estimate the patient effort of asynchronous breathing. It is shown that even in case of patient-ventilator asynchrony the algorithm is able to retrieve accurate estimates.

The first results is the improved estimation of the patient parameters as shown in Fig. 5. The solid blue line in this figure represents the normalized true parameter and the dashed lines represent a 15% accuracy interval. The red markers in Fig. 5 show the estimated parameters for every patient using the least-squares estimator assuming zero patient effort, the green markers show the estimated parameters for every patient using the proposed algorithm. Furthermore, on the horizontal axis

the depth of the patient effort is given, corresponding to the plots in Fig. 4. Note that for the case of no patient effort the red markers are exactly underneath the green markers. It is clearly seen that when there is no effort, i.e., breath depth is 0 mbar, all estimates are close to the true parameter. For an increasing breath depth, the estimates of the least square estimator assuming zero patient effort deviate from the true parameters and are clearly outside the desired 15% accuracy interval. The effect of the breath depth on the estimated parameters is much smaller when using the proposed algorithm in (9). The parameters are slightly diverging, caused by the bias due to the regularization term, but remain very close to the true parameters. In conclusion, the proposed algorithm significantly outperforms the least-squares estimator assuming zero patient efforts.

The second result is the estimation of the patient effort as shown in Fig. 4. This figure shows the true effort for every experiment in blue, the assumed effort for the estimator assuming zero effort in red, and the estimated effort for the proposed algorithm in green. It is clearly seen in case of no effort, i.e., the top plot, the proposed method retrieves the true effort and the assumption by the benchmark algorithm is correct as well. When increasing the patient effort, the zero effort assumption in the least-squares estimator is clearly wrong. Note that one might propose the following, rather naive, approach to estimate the patient effort. Use the estimated values of C_{lung} and R_{lung} which are obtained using the least-squares estimator under the assumption $p_{mus}(k) = 0 \forall k \geq 0$. Then, compute the patient's breathing effort using the residual estimation error, i.e., $p_{mus}(k) = p_{aw}(k) - (\frac{1}{\hat{C}_{lung}}V_{pat}(k) + \hat{R}_{lung}Q_{pat}(k) + \hat{p}_{lung}(1))$. However, the estimated parameters already aim to capture this patient effort. Therefore, extensive testing has shown that $p_{mus}(k) = 0$ is a significantly better estimate of the actual effort. Furthermore, it is observed that the proposed algorithm estimates the patient effort almost perfectly in these simulations. Only a small bias is introduced by the regularization term in (9).

This bias in the parameter and the patient effort estimates can be reduced by applying re-estimation, as explained in Section IV. This re-estimation method is omitted for brevity and clarity of this paper.

Finally, to analyze the performance of the proposed algorithm over a wide variety of patients and ventilator settings Monte Carlo simulations have been conducted. In this analysis, the following parameters are sampled from a uniformly distributed set as indicated:

- $C_{lung} \in [10, 60]$ ml/mbar;
- $R_{lung} \in [5, 20]$ mbar/l/s;
- $\min(p_{mus}(k)) \in [0, 10]$ mbar;
- IPAP $\in [15, 30]$ mbar.

The results of this Monte Carlo study are visualized in Fig. 6. The figure shows the normalized compliance and resistance estimates for both algorithms. It clearly shows that the proposed algorithm with ℓ_1-regularization outperforms the least-squares estimator. Furthermore, it shows that the
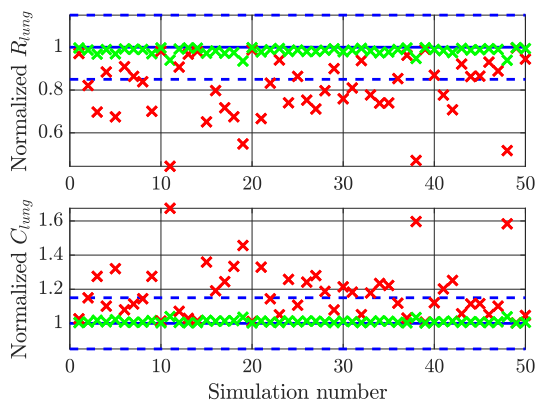
FIGURE 6. Normalized estimates of the Monte Carlo study showing the results of the least-squares estimator assuming zero effort (✗) and the estimates of the proposed algorithm with ℓ_1-regularization (✗). The figure clearly shows that the proposed algorithm acurately estimates the true parameters over a wide variety of scenarios.
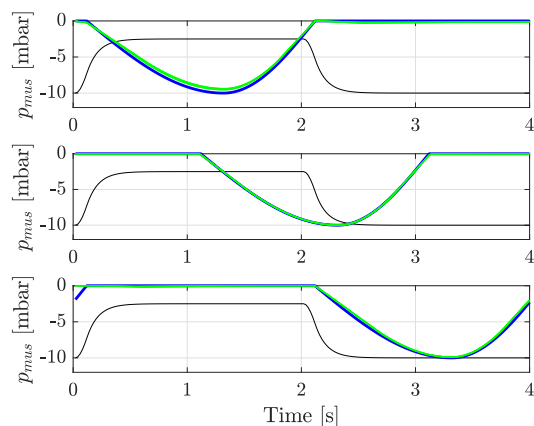

FIGURE 7. The true and estimated effort for every patient in simulations with asynchronous breathing. Every figure shows the true breathing effort (▬▬▬), the estimated effort using the presented approach (▬▬▬), and a scaled version of the target pressure (▬▬▬) to indicate the asynchrony.

algorithm obtains accurate estimates for a wide variety of scenarios.

In conclusion, these simulation results show that the proposed algorithm retrieves useful estimates of the patient parameters and the patient effort. In contrast, the parameter estimates of the method assuming zero patient effort diverge significantly when patient effort is present, rendering these estimates inaccurate.

C. SIMULATION RESULTS ASYNCRHONY

Patient-ventilator asynchrony typically renders such estimation problems highly challenging. Therefore, a simulation study is carried out to show that the proposed estimation algorithm is robust against these asynchronies. The results of this study are shown in Fig. 7. The top plot shows the synchronized use-cases from the previous section and the middle and bottom plot show the estimation results for asynchronous breathing. These results show that the proposed algorithm
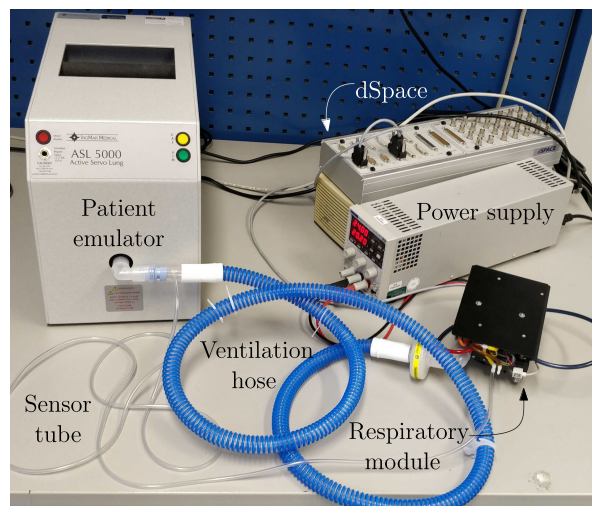

FIGURE 8. The experimental setup showing the main components: the patient emulator, respiratory module, ventilation hose, dSpace module, and power supply.

retrieves accurate estimates of the patient effort in this simulation study of patient-ventilator asynchrony.

VI. EXPERIMENTAL CASE STUDY

In this section, the proposed algorithm is validated through an experimental study. First of all, in Section VI-A, the used experimental setup and use-cases are described. Thereafter, the estimation results are presented and analyzed in Section VI-B.

A. EXPERIMENTAL SETUP DESCRIPTION

The main components of the experimental setup used in this case study are depicted in Fig. 8. The figure shows the blower-driven mechanical ventilation module of Demcon macawi respiratory systems [41]. The airway pressure p_{aw} is measured using the sensor tube and a gauge pressure sensor inside the respiratory module. The patient flow Q_{pat} is estimated based on the measured airway pressure and a leak model obtained through a calibration routine. The ventilator is attached to a dSPACE system (dSPACE GmbH, Paderborn, Germany), where the controls are implemented using MATLAB Simulink (MathWorks, Natick, MA) running at a sampling frequency of 500 Hz. Note that data sampling for estimation is done at 50 Hz, similar to the simulations. This is done to reduce the required memory, which is limited on a typical ventilation system.

Furthermore, the ASL 5000^{TM} Breathing Simulator (IngMar Medical, Pittsburgh, PA) represents the patient. This lung simulator can be used to emulate a wide variety of patients with a linear resistance and compliance. Furthermore, it is able to simulate predefined breathing effort.

Exactly the same settings as in the simulation case study in Section V are used. More specifically, the breathing simulator is set to emulate the same patients and patient effort that are considered in the simulations case-study. Furthermore,
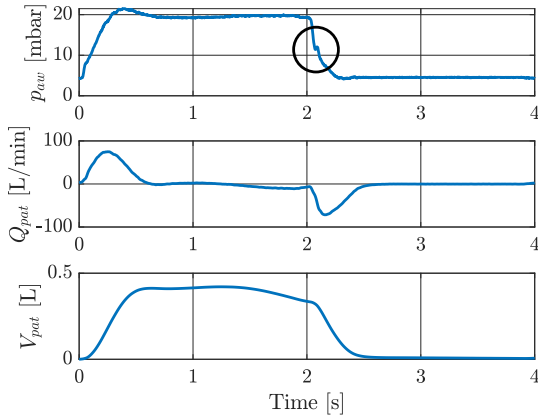
FIGURE 9. Raw measured data of the patient use case R5C20 with a breath depth of 5 mbar. The figure displays the airway pressure p_{aw}, the patient flow Q_{pat}, and the patient volume V_{pat}.
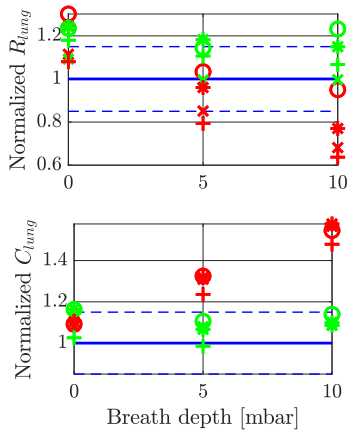

FIGURE 10. The normalized values of the estimated parameters $\hat{R}_{lung}$ and $\hat{C}_{lung}$ for the different patients against the breath depths in experiments. The figures show the true normalized parameters (———), the 15% accuracy interval (– – –), the estimated parameters neglecting the patient effort in red, and the estimated parameters using the presented approach in green. Four different patient types are considered namely: R5C20 (O), R10C20 (×), R5C50 (*), and R10C50 (+).

the ventilator generates a PEEP and IPAP of 5 and 20 mbar, respectively. The ventilator's inspiration is triggered by a flow trigger induced by the patient effort. Then, after two seconds the ventilator cycles off to PEEP.

An example of the measured raw data is depicted in Fig. 9, this figure shows the measured data of a patient with resistance of 5 mbar/l/s and a compliance of 20 ml/mbar, with a breath depth of 5 mbar. The figure shows the airway pressure p_{aw}, the patient flow Q_{pat}, and the patient volume V_{pat}.

B. EXPERIMENTAL RESULTS

The main results of the experiments are shown in Fig. 10 and 11. Next, the results for the estimated parameters and the estimated patient effort are analyzed separately.
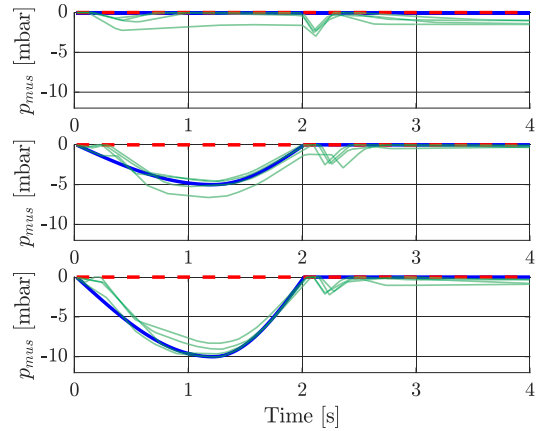

FIGURE 11. The true and estimated effort for every patient in experiments. From top to bottom the figures show the patients with a breath depth of 0, 5, and 10 mbar, respectively. The figures show the patient effort (———), the patient effort considered by the algorithm assuming $p_{mus} = 0$ (– – –), and the estimated effort using the presented approach (———).

First, the results of the estimated parameters are investigated. Fig. 10 shows the normalized estimated parameter. In general it shows similar results to the simulation results in Fig. 5. The parameters obtained with the least-squares estimator assuming zero patient effort are diverging when increasing the patient effort and the estimates with the proposed method remain significantly more accurate.

The main difference with the simulations is that the resistance estimate without effort shows a significant offset from the "true" value, also in case of a least-squares estimation where $\hat{p}_{mus} = 0$, i.e., the true effort. This is caused by tubing between the sensors of the module, which are used for estimation, and the sensors of the ASL 5000, which are used internally by the ASL 5000 to emulate the desired behavior. This additional tubing results in a slightly increased resistance.

Second, results of the estimated patient effort are analyzed. Fig. 11 shows the true effort for every experiment in blue, the assumed effort for the traditional least-squares estimator in red, and the estimated effort for the proposed algorithm in green. It is clearly seen in case of no effort, i.e., the top plot, the estimates using the algorithm in (9) retrieves effort close to zero. However, there is some slight deviation. When increasing the effort, the proposed algorithm retrieves an accurate estimate of the true effort, which is highly useful in practice. It seems that the regularization term in (9) introduces bias in the estimates. Furthermore, at about 2 seconds, a slight spike in the estimated effort is observed. This happens at the start of the expiration of the ventilator. It is likely that this spike is caused by the ASL 5000. It is seen that it takes some time for the ASL 5000 to respond to the pressure change that is introduced by the ventilator-induced expiration. This artifact is clearly visible in the circle of the measured airway pressure in Fig. 9.
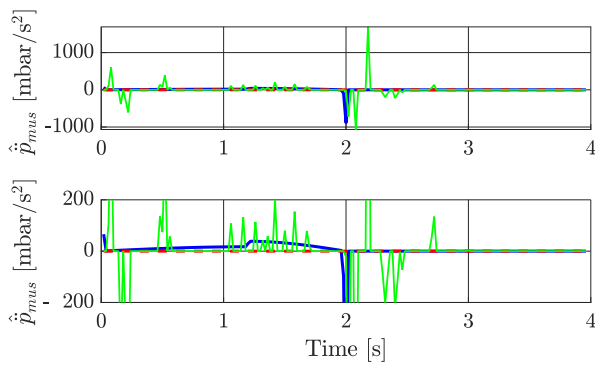
FIGURE 12. The second time derivative of the patient effort $\ddot{p}_{mus}$ for the R5C20 patient with a breath depth of 20 mbar. With two different scales on the vertical axis to clearly show the sparsity property. Showing the true value (——), the value considered by the algorithm assuming $p_{mus} = 0$ (– – –), and the estimated value using the presented approach (——).

Finally the sparsity of the estimated effort is analyzed in Fig. 12. This figure shows the second time derivative of the estimated patient effort $\ddot{p}_{mus}$ in one particular use-case, with two different scales on the vertical axis. The figure clearly shows that a sparse estimate is retrieved, since many values are zero. Furthermore, it shows that the spike caused by the ASL 5000 causes significant spikes in $\ddot{p}_{mus}$. This spike is quickly compensated by another spike. Therefore, the effect on the estimate patient effort $\hat{p}_{mus}$ is not as significant.

Concluding, this experimental case study shows that the proposed algorithm retrieves estimates of the patient parameters and the patient effort that are significantly more accurate than the parameters obtained by the traditional least-squares estimator. Therefore, the retrieved parameters and patient effort can be used by a clinician to improve the patient's treatment.

VII. CONCLUSIONS AND RECOMMENDATIONS

In this paper, an estimation framework is presented that can help to identify a ventilated patient's clinical condition. This is achieved by a sparse parameter estimation method to retrieve estimates of relevant patient parameters and the patient effort of a spontaneously breathing mechanically ventilated patient.

The estimation problem, with the available sensors, is non-identifiable. This had to be overcome without interfering with the patient's regular treatment. This is achieved by embedding prior knowledge of the patient effort in the estimation problem. More specifically, that the patient effort cannot change arbitrarily, i.e., its second time derivative is sparse. Embedding this sparsity property in the optimization problem by means of an ℓ_1-regularization term results in a convex optimization problem that retrieves realistic estimates.

The proposed method is validated by means of simulation and experimental case studies. Through these case studies, it is shown that the presented algorithm retrieves realistic and useful estimates of the patient parameters and patient effort

in a specific mode of triggered ventilation. The retrieved estimates can be used by clinicians to determine the patient's clinical condition and optimize the treatment.

Several recommendations are considered relevant for future extensions. First, to validate that the algorithm gives clinically useful and realistic estimates in a practical setting, the algorithm should be tested on actual patient data. Second, the algorithm outcome should be compared to existing methods that give an indication about the patient effort, such as, the P0.1 test. Third, the current algorithm does not work in all modes of ventilation, e.g., Continuous Positive Airway Pressure (CPAP) ventilation. Therefore, more research is required to develop an algorithm that works in other modes of ventilation. Fourth, methods such as re-estimation [29] or reweighting [35] could be considered to improve estimation quality further in future work. Fifth, the algorithm should be further developed to improve estimation when deviating from the nominal cases presented in this paper. For example, the algorithm's estimation performance should be improved in case of an active expiration. Finally, using clinical data of ventilated patients with an esophageal pressure measurement, a method to optimally choose the regularization parameter λ should be developed.

REFERENCES

[1] M. A. Warner and B. Patel, "Mechanical ventilation," in *Benumof and Hagberg's Airway Management*. Amsterdam, The Netherlands: Elsevier, 2013, pp. 981–997.

[2] C. R. Wells *et al.*, "Projecting the demand for ventilators at the peak of the COVID-19 outbreak in the USA," *Lancet Infect. Dis.*, vol. 20, no. 10, pp. 1123–1125, Apr. 2020.

[3] J. H. T. Bates, *Lung Mechanics*. Cambridge, U.K.: Cambridge Univ. Press, 2009.

[4] M. Borrello, "Adaptive inverse model control of pressure based ventilation," in *Proc. IEEE Amer. Control Conf.*, 2001, pp. 1286–1291.

[5] G. Avanzolini, P. Barbini, A. Cappello, G. Cevenini, and L. Chiari, "A new approach for tracking respiratory mechanical parameters in real-time," *Ann. Biomed. Eng.*, vol. 25, no. 1, pp. 154–163, Jan. 1997.

[6] L. Blanch *et al.*, "Asynchronies during mechanical ventilation are associated with mortality," *Intensive Care Med.*, vol. 41, no. 4, pp. 633–641, Feb. 2015.

[7] D. M. Needham, S. E. Bronskill, J. R. Calinawan, W. J. Sibbald, P. J. Pronovost, and A. Laupacis, "Projected incidence of mechanical ventilation in Ontario to 2026: Preparing for the aging baby boomers," *Crit. Care Med.*, vol. 33, no. 3, pp. 574–579, Mar. 2005.

[8] D. C. Angus, M. A. Kelley, R. J. Schmitz, A. White, and J. Popovich, "Current and projected workforce requirements for care of the critically ill and patients with pulmonary disease," *JAMA*, vol. 284, no. 21, pp. 2762–2770, 2000.

[9] P. Navalesi and R. Costa, "New modes of mechanical ventilation: Proportional assist ventilation, neurally adjusted ventilatory assist, and fractal ventilation," *Curr. Opin. Crit. Care*, vol. 9, no. 1, pp. 51–58, Feb. 2003.

[10] C. Sinderby *et al.*, "Neural control of mechanical ventilation in respiratory failure," *Nature Med.*, vol. 5, no. 12, pp. 1433–1436, Dec. 1999.

[11] C. Sinderby and J. Beck, "Proportional assist ventilation and neurally adjusted ventilatory assistbetter approaches to patient ventilator synchrony?," *Clin. Chest Med.*, vol. 29, no. 2, pp. 329–342, Jun. 2008.

[12] J. Doorduin, H. W. H. van Hees, J. G. van der Hoeven, and L. M. A. Heunks, "Monitoring of the respiratory muscles in the critically ill," *Amer. J. Respir. Crit. Care Med.*, vol. 187, no. 1, pp. 20–27, Jan. 2013.

[13] E. Petersen, J. Graßhoff, M. Eger, and P. Rostalski, "Surface EMG-based estimation of breathing effort for neurally adjusted ventilation control," in *Proc. 21st IFAC World Congr.*, 2020, pp. 16323–16328.

[14] D. Navajas, J. Alcaraz, R. Peslin, J. Roca, and R. Farré, "Evaluation of a method for assessing respiratory mechanics during noninvasive ventilation," *Eur. Respir. J.*, vol. 16, pp. 704–709, Oct. 2000.

[15] F. Dietz, A. Schloßer, and D. Abel, "Flow controlled non-invasive ventilation considering mask leakage and spontaneous breathing," *IFAC Proc. Volumes*, vol. 36, no. 16, pp. 151–156, Sep. 2003.

[16] H. Maes, G. Vandersteen, M. Muehlebach, and C. Ionescu, "A fan-based, low-frequent, forced oscillation technique apparatus," *IEEE Trans. Instrum. Meas.*, vol. 63, no. 3, pp. 603–611, Mar. 2014.

[17] H. Maes, M. Zivanovic, J. Schoukens, and G. Vandersteen, "Estimating respiratory impedance at breathing frequencies using regularized least squares on forced oscillation technique measurements," *IEEE Trans. Instrum. Meas.*, vol. 66, no. 3, pp. 479–491, Mar. 2017.

[18] H. Maes, G. Vandersteen, and C. Ionescu, "Estimation of respiratory impedance at low frequencies during spontaneous breathing using the forced oscillation technique," in *Proc. 36th Annu. Int. Conf. IEEE Eng. Med. Biol. Soc.*, 2014, pp. 3410–3413.

[19] C. Ionescu, J. Schoukens, and R. D. Keyser, "Detecting and analyzing non-linear effects in respiratory impedance measurements," in *Proc. 2011 Amer. Control Conf.*, 2011, pp. 5412–5417.

[20] M. Ghita, D. Copot, M. Ghita, E. Derom, and C. Ionescu, "Low frequency forced oscillation lung function test can distinguish dynamic tissue non-linearity in COPD patients," *Front. Physiol.*, vol. 10, Nov. 2019, Art. no. 1390.

[21] N. S. Damanhuri *et al.*, "Assessing respiratory mechanics using pressure reconstruction method in mechanically ventilated spontaneous breathing patient," *Comput. Methods Prog. Biomed.*, vol. 130, pp. 175–185, Jul. 2016.

[22] J. L. Knopp, J. G. Chase, K. T. Kim, and G. M. Shaw, "Model-based estimation of negative inspiratory driving pressure in patients receiving invasive NAVA mechanical ventilation," *Comput. Methods Prog. Biomed.*, vol. 208, Sep. 2021, Art. no. 106300.

[23] F. Vicario, A. Albanese, N. Karamolegkos, D. Wang, A. Seiver, and N. Chbat, "Noninvasive estimation of respiratory mechanics in spontaneously breathing ventilated patients: A constrained optimization approach," *IEEE Trans. Biomed. Eng.*, vol. 63, no. 4, pp. 775–787, Apr. 2016.

[24] D. P. Redmond, Y. S. Chiew, V. Major, and J. G. Chase, "Evaluation of model-based methods in estimating respiratory mechanics in the presence of variable patient effort," *Comput. Methods Prog. Biomed.*, vol. 171, pp. 67–79, Apr. 2019.

[25] C. Olivieri, R. Costa, G. Conti, and P. Navalesi, "Bench studies evaluating devices for non-invasive ventilation: Critical analysis and future perspectives," *Intensive Care Med.*, vol. 38, no. 1, pp. 160–167, Nov. 2011.

[26] E. Fresnel, J.-F. Muir, and C. Letellier, "Realistic human muscle pressure for driving a mechanical lung," *EPJ Nonlinear Biomed. Phys.*, vol. 2, no. 1, Aug. 2014, Art. no. 7.

[27] R. Tibshirani, "Regression shrinkage and selection via the LASSO," *J. Roy. Stat. Soc.: Ser. B. (Methodological)*, vol. 58, no. 1, pp. 267–288, Jan. 1996.

[28] R. Tibshirani, M. Saunders, S. Rosset, J. Zhu, and K. Knight, "Sparsity and smoothness via the fused lasso," *J. Roy. Stat. Soc.: Ser. B. (Stat. Methodol.)*, vol. 67, no. 1, pp. 91–108, Feb. 2005.

[29] T. Oomen and C. R. Rojas, "Sparse iterative learning control with application to a wafer stage: Achieving performance, resource efficiency, and task flexibility," *Mechatronics*, vol. 47, pp. 134–147, Nov. 2017.

[30] H. Ohlsson, L. Ljung, and S. Boyd, "Segmentation of ARX-models using sum-of-norms regularization," *Automatica*, vol. 46, no. 6, pp. 1107–1111, Jun. 2010.

[31] C. R. Rojas and H. Hjalmarsson, "Sparse estimation based on a validation criterion," in *Proc. IEEE Conf. Decis. Control Eur. Control Conf.*, 2011, pp. 2825–2830.

[32] Y. S. Chiew *et al.*, "Time-varying respiratory system elastance: A physiological model for patients who are spontaneously breathing," *PLoS One*, vol. 10, no. 1, Jan. 2015, Art. no. e0114847.

[33] E. J. van Drunen *et al.*, "Visualisation of time-varying respiratory system elastance in experimental ARDS animal models," *BMC Pulmonary Med.*, vol. 14, no. 1, Mar. 2014, Art. no. 33.

[34] B. K. Natarajan, "Sparse approximate solutions to linear systems," *SIAM J. Comput.*, vol. 24, no. 2, pp. 227–234, Apr. 1995.

[35] E. J. Candès, M. B. Wakin, and S. P. Boyd, "Enhancing sparsity by reweighted ℓ_1 minimization," *J. Fourier Anal. Appl.*, vol. 14, no. 5/6, pp. 877–905, Oct. 2008.

[36] K. Murphy, *Machine Learning: A Probabilistic Perspective*. Cambridge, Mass, U.K.: MIT Press, 2012.

[37] E. J. Candes and T. Tao, "Decoding by linear programming," *IEEE Trans. Inf. Theory*, vol. 51, no. 12, pp. 4203–4215, Dec. 2005.

[38] M. Grant and S. Boyd, "Graph implementations for nonsmooth convex programs," in *Recent Advances in Learning and Control, Ser. Lecture Notes in Control and Information Sciences*, V. Blondel, S. Boyd, and H. Kimura, Eds. Berlin, Germany: Springer-Verlag, 2008, pp. 95–110. [Online]. Available: http://stanford.edu/boyd/graph_dcp.html

[39] M. Grant and S. Boyd, "CVX: Matlab software for disciplined convex programming, version 2.1," Mar. 2014. [Online]. Available: http://cvxr.com/cvx

[40] J. Reinders, B. Hunnekens, F. Heck, T. Oomen, and N. van de Wouw, "Adaptive control for mechanical ventilation for improved pressure support," *IEEE Trans. Control Syst. Technol.*, vol. 29, no. 1, pp. 180–193, Jan. 2021.

[41] DEMCON macawi respiratory systems, "OEM solutions," Accessed: Oct. 19, 2020. [Online]. Available: https://www.macawi.com/products-services/

JOEY REINDERS was born in 1994. He received the B.Sc. and M.Sc. degrees in mechanical engineering from Eindhoven University of Technology, Eindhoven, The Netherlands, in 2015 and 2017, respectively. In 2022, he received the Ph.D. degree from DEMCON Advanced Mechatronics, Best, The Netherlands, in collaboration with the Dynamics and Control Group, Department of Mechanical Engineering, Eindhoven University of Technology. During his Ph.D. research, he developed learning control and identification algorithms for mechanical ventilation. Currently, he is working at DEMCON Advanced Mechatronics on the development of medical devices as a System Engineer.

BRAM HUNNEKENS was born on May 22, 1987. He recieved the B.Sc. and M.Sc degrees (cum laude) in mechanical engineering from the Eindhoven University of Technology, the Netherlands, in 2008 and 2011, respectively. In 2015, he obtained the Ph.D. degree in mechanical engineering for his thesis "Performance optimization of hybrid controllers for linear motion systems." In 2016, he was the recipient of the DISC "Best Thesis Award." Currently, he is affiliated with Demcon in the role of System Engineer. His main research interests include nonlinear control, performance, high-tech systems, medical systems, and mechanical ventilation.

NATHAN VAN DE WOUW (Fellow, IEEE) was born in 1970. He received the M.Sc. (with Hons.) and Ph.D. degrees in mechanical engineering from the Eindhoven University of Technology, Eindhoven, The Netherlands, in 1994 and 1999, respectively. He is currently a Full Professor with the Mechanical Engineering Department, Eindhoven University of Technology. In 2000, he was with Philips Applied Technologies, Eindhoven, The Netherlands, and in 2001, was with the Netherlands Organisation for Applied Scientific Research (TNO), Delft, The Netherlands. He was a Visiting Professor with the University of California Santa Barbara, Santa Barbara, CA, USA, in 2006/2007, with University of Melbourne, Parkville, VIC, Australia, in 2009/2010, and with University of Minnesota, Minneapolis, MN, USA, in 2012 and 2013. He was a (part-time) Full Professor with the Delft University of Technology, The Netherlands, from 2015 to 2019. He was an Adjunct Full Professor with the University of Minnesota, from 2014 to 2021. He has authored or coauthored the books "*Uniform Output Regulation of Nonlinear Systems: A convergent Dynamics Approach*" with A.V. Pavlov and H. Nijmeijer (Birkhauser, 2005) and "*Stability and Convergence of Mechanical Systems with Unilateral Constraints*" with R.I. Leine (Springer-Verlag, 2008). His research interests include the modelling, model reduction, analysis and control of nonlinear/hybrid and delay systems, with applications to autonomous and cooperative driving, high-tech systems, resource exploration, health applications, and cyber-physical systems. Dr. van de Wouw was on the Editorial Board for the journals *Automatica*, IEEE TRANSACTIONS ON CONTROL SYSTEMS TECHNOLOGY, and IEEE TRANSACTIONS ON AUTOMATIC CONTROL. He is a Fellow for his contributions to hybrid, data-based and networked control, and in 2015, he was the recipient of the IEEE Control Systems Technology Award for the development and application of variable-gain control techniques for high-performance motion systems.

TOM OOMEN (Senior Member, IEEE) received the M.Sc. (cum laude) and Ph.D. degrees from the Eindhoven University of Technology, Eindhoven, The Netherlands. He is Full Professor with the Department of Mechanical Engineering at the Eindhoven University of Technology. He is also a part-time Full Professor with the Delft University of Technology. He held visiting positions at KTH, Stockholm, Sweden, and at The University of Newcastle, Australia. He is a recipient of the 7th Grand Nagamori Award, the Corus Young Talent Graduation Award, the IFAC 2019 TC 4.2 Mechatronics Young Research Award, the 2015 IEEE TRANSACTIONS ON CONTROL SYSTEMS TECHNOLOGY Outstanding Paper Award, the 2017 IFAC Mechatronics Best Paper Award, the 2019 IEEE JOURNAL OF INDUSTRY APPLICATIONS Best Paper Award, and recipient of a Veni and Vidi personal grant. He is Associate Editor of the IEEE CONTROL SYSTEMS LETTERS (L-CSS), *IFAC Mechatronics*, IEEE TRANSACTIONS ON CONTROL SYSTEMS TECHNOLOGY, and has been vice-chair for IFAC TC 4.2. He is a member of the Eindhoven Young Academy of Engineering. His research interests are in the field of data-driven modeling, learning, and control, with applications in precision mechatronics.